

## Voxel-based analyses of magnetization transfer imaging of the brain in hepatic encephalopathy

Falk R Miese, Hans-Jörg Wittsack, Gerald Kircheis, Arne Holstein, Christian Mathys, Ulrich Mödder, Mathias Cohnen

Falk R Miese, Hans-Jörg Wittsack, Arne Holstein, Christian Mathys, Ulrich Mödder, Mathias Cohnen, Institute of Radiology, University Hospital Düsseldorf, MNR Clinic, Moorenstrasse 5, Düsseldorf 40225, Germany

Gerald Kircheis, Department of Internal Medicine, Division of Gastroenterology, Hepatology and Infectious Diseases, University Hospital Düsseldorf, Moorenstrasse 5, Düsseldorf 40225, Germany

Author contributions: Miese FR, Wittsack HJ, Kircheis G, Holstein A, Mödder U and Cohnen M designed the research; Miese FR, Wittsack HJ, Kircheis G and Mathys C performed the research; Miese FR, Wittsack HJ and Holstein A analyzed the data; Miese FR wrote the paper.

Correspondence to: Dr. Falk R Miese, Institute of Radiology, University Hospital Düsseldorf, MNR Clinic, Moorenstrasse 5, Düsseldorf 40225, Germany. [dr.miese@gmx.de](mailto:dr.miese@gmx.de)

Telephone: +49-211-8117752 Fax: +49-211-8116145

Received: May 27, 2009 Revised: August 3, 2009

Accepted: August 10, 2009

Published online: November 7, 2009

**CONCLUSION:** The distribution of MTR changes in HE points to an early involvement of basal ganglia and white matter in HE.

© 2009 The WJG Press and Baishideng. All rights reserved.

**Key words:** Brain; Hepatic encephalopathy; Magnetic resonance imaging; Liver cirrhosis; Magnetization transfer imaging

**Peer reviewers:** Paul E Sijens, PhD, Associate Professor, Radiology, UMCG, Hanzeplein 1, 9713GZ Groningen, The Netherlands; Diego Garcia-Compean, MD, Professor, Faculty of Medicine, University Hospital, Department of Gastroenterology, Autonomous University of Nuevo Leon, Ave Madero y Gonzalitos, 64700 Monterrey, NL, México

Miese FR, Wittsack HJ, Kircheis G, Holstein A, Mathys C, Mödder U, Cohnen M. Voxel-based analyses of magnetization transfer imaging of the brain in hepatic encephalopathy. *World J Gastroenterol* 2009; 15(41): 5157-5164 Available from: URL: <http://www.wjgnet.com/1007-9327/15/5157.asp> DOI: <http://dx.doi.org/10.3748/wjg.15.5157>

### Abstract

**AIM:** To evaluate the spatial distribution of cerebral abnormalities in cirrhotic subjects with and without hepatic encephalopathy (HE) found with magnetization transfer imaging (MTI).

**METHODS:** Nineteen cirrhotic patients graded from neurologically normal to HE grade 2 and 18 healthy control subjects underwent magnetic resonance imaging. They gave institutional-review-board-approved written consent. Magnetization transfer ratio (MTR) maps were generated from MTI. We tested for significant differences compared to the control group using statistical non-parametric mapping (SnPM) for a voxel-based evaluation.

**RESULTS:** The MTR of grey and white matter was lower in subjects with more severe HE. Changes were found in patients with cirrhosis without neurological deficits in the basal ganglia and bilateral white matter. The loss in magnetization transfer increased in severity and spatial extent in patients with overt HE. Patients with HE grade 2 showed an MTR decrease in white and grey matter: the maximum loss of magnetization transfer effect was located in the basal ganglia [SnPM (pseudo-) $t = 17.98$ ,  $P = 0.0001$ ].

### INTRODUCTION

Hepatic encephalopathy (HE) is a frequent complication of liver cirrhosis, which is characterized by sleeping disorders, asterixis, and deficits in motor skills and reaction time. Twenty to eighty percent of patients with cirrhosis suffer from minimal HE (mHE)<sup>[1]</sup>. Five years after the diagnosis of mHE, 26% of patients with liver cirrhosis have episodes of overt HE. This condition is associated with a poor prognosis<sup>[2]</sup>.

Studies using magnetization transfer contrast imaging (MTI) have demonstrated a decrease in the magnetization transfer ratio (MTR) in the brains of cirrhosis patients with mHE and overt HE<sup>[3-10]</sup>. MTR decrease in cirrhosis has been proposed to be an effect of astrocytic water retention<sup>[5-7,9,10]</sup>, demyelination<sup>[5]</sup> and axonal loss<sup>[5]</sup>, in addition to changes in blood flow and energy metabolism<sup>[9]</sup>.

MTI has been used successfully to monitor normalization of cerebral abnormalities in cirrhosis patients following liver transplantation<sup>[8]</sup>, and has been shown to detect increasing abnormalities following induced hyperammonemia<sup>[9]</sup>.

The cited studies evaluated MTR maps using region-of-interest (ROI) based analyses. The MTR of normal appearing white matter<sup>[5-10]</sup> and anatomically defined areas of deep grey matter<sup>[3-5,10]</sup> have been the subject of previous studies on HE. To the best of our knowledge, no systematic evaluation of the spatial distribution of MTR abnormalities in HE has been published so far. The purpose of the present study is to evaluate the spatial distribution of MTI changes caused by central nervous system (CNS) abnormalities in HE.

## MATERIALS AND METHODS

### Subjects

Approval was obtained from the institution's review board. All patients and volunteers gave written informed consent after the neuropsychological tests and magnetic resonance imaging (MRI) had been explained fully. In this prospective study (for details see Table 1), 19 patients (14 male and five female) with non-alcoholic cirrhosis and 18 age-matched controls (eight male and 10 female) were included. Cirrhosis was caused by hepatitis C ( $n = 9$ ), hemochromatosis ( $n = 2$ ), primary chronic cholangitis ( $n = 2$ ), hepatitis B ( $n = 1$ ), Wilson's disease ( $n = 1$ ) and cryptogenic cirrhosis ( $n = 4$ ).

Subjects with a history of drug abuse, including alcohol, and those suffering from neurological or psychiatric diseases were excluded. Also excluded were patients who were taking CNS-relevant medications such as benzodiazepines, benzodiazepine antagonists and antidepressants. Further exclusion criteria were severe diseases such as spontaneous bacterial peritonitis, severe renal failure, uncontrolled diabetes mellitus or coronary heart disease. Since asterixis and hyperreflexia, as well as other more severe neurological conditions such as stupor or somnolence may interfere with safe and artefact-free MRI, patients with higher degrees of HE (grade 3 or 4) who also had these conditions were not considered for investigation. Also, patients needed to cooperate for neuropsychological examination and the patients' willingness represented a limitation in testing subjects with HE grade 3 or 4.

The severity of liver disease was determined according to the Child-Pugh-score<sup>[11]</sup>: patients were graded Child-Pugh A in nine cases, B in five and C in five.

### Neuropsychological examination

Five computerized psychometric neurological tests were performed on each patient. The test battery included the visual pursuit test, motor performance series, Cognitron, Vienna reaction test and Tachistoscopic Traffic Test Mannheim for Screen (TAVTMB) as part of the Vienna Test System (Schuhfried GmbH, Mödling, Austria, 1999). mHE was diagnosed if a patient showed no clinical overt symptoms of HE and performed at  $< 1$  SD below the mean in at least two of the five computer psychometric tests of the test battery. Cirrhosis patients without clinical overt HE who performed at  $< -1$  SD in only one of the tests were graded as having no HE<sup>[12]</sup>. Overt encephalopathy was graded according to the

**Table 1** Nineteen patients with cirrhosis and 18 controls were enrolled (mean  $\pm$  SD)

	Controls	Cirrhosis
<i>n</i> (male/female)	18 (8/10)	19 (14/5)
Age (yr)	55.7 $\pm$ 13.8	61.1 $\pm$ 12.4 NS
CFF (Hz)	41.3 $\pm$ 1.6	36.6 $\pm$ 4.9 <sup>b</sup>
Child-Pugh grading		
A		9
B		5
C		5
HE grading		
HE 0		5
mHE		3
HE 1		6
HE 2		5

<sup>b</sup> $P < 0.01$  vs controls (Mann-Whitney *U* test). NS: No significant difference.

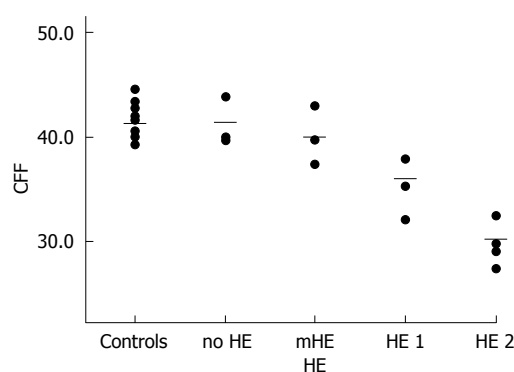


**Figure 1** CFF of controls and patients. HE grading and CFF (Hz). Circles indicate individuals' CFF, bars represent means of groups (mean CFF of controls: 41.3 Hz; mean CFF of group with no HE: 41.4 Hz; mean CFF of group with mHE: 40.0 Hz; mean CFF of group with HE 1: 36.1 Hz; mean CFF of group with HE 2: 30.2 Hz).

West-Haven criteria<sup>[13]</sup>. Cirrhosis patients were graded as no HE in five cases, mHE in three, HE 1 in six and HE 2 in five cases (Table 1).

In order to assess the severity of HE, the critical flicker frequency (CFF) was introduced in 2002. CFF is used in the evaluation of neurological deficits in low-grade HE and has been shown to respond readily to an improvement or deterioration of neurological symptoms<sup>[12]</sup>.

CFF was determined in each patient using the Schuhfried Test System (Eberhard, G. Schuhfried GmbH, Mödling, Austria, 1994). A flickering light of 650 nm wavelength and 5.3 mcd was used for intrafoveal stimulation, while the flickering frequency decreased at 0.5-0.01 Hz/s. The CFF was defined as the frequency needed to perceive initially the stimulus as non-continuous. The means of eight repeat tests were determined (Figure 1).

### MRI protocol

All scans were acquired on a 1.5-T clinical scanner (Magnetom Vision Plus; Siemens Medical Solutions, Erlangen, Germany) using the standard head coil. MTI was performed with two 2D gradient-echo sequences (TR 700 ms, TE 12 ms, flip angle  $\alpha = 20^\circ$ , one acquisition, 20 slices of 5 mm thickness, 0.5 mm gap), using a matrix

of  $224 \times 256$  pixels with a field of view of  $240 \text{ mm} \times 240 \text{ mm}$ . The first set of images was obtained with no saturation pulse. The latter sequence used a saturation pulse 1.5 kHz below  $\text{H}_2\text{O}$  frequency, with a bandwidth of 250 Hz, 7.68 ms length and a flip angle of  $500^\circ$ . Additionally, routine examinations including T2- and T1-weighted imaging were performed to exclude patients with asymptomatic infarction or chronic ischemic changes.

### Image processing

For each subject, the MTR was quantified as a percentage of signal loss between the two images according to the following equation:  $\text{MTR} = (S_0 - S_s)/S_0 \times 100\%$ .  $S_0$  is the mean signal intensity of a pixel obtained from the sequence using no saturation pulse, and  $S_s$  is the mean signal intensity with the applied saturation pulse. Gray values in these secondary images represent MTR data, which yielded an MTR map.

Pixels that contained skull and soft tissue in the MTR maps were removed using the MRIcro-Software<sup>[14]</sup>. Images without skull and soft tissue pixels were used, since this has been reported to improve the validity of voxel-based evaluation of brain imaging data<sup>[14]</sup>.

The MTR maps that contained only brain pixels were normalized into a standardized space using statistical parametric mapping (SPM5) software<sup>[15]</sup>. An MTR template was generated to ensure reliable normalization. For this, the images of all individuals were smoothed with a Gaussian kernel of 3 mm full width at half maximum, and normalized to the standard SPM EPI-template (Montreal Neurological Institute). The mean of the 37 normalized images was used as an MTR template for the normalization of each original MTR map. The default spatial normalization settings were applied. A Gaussian kernel of 3 mm full width at half maximum was used for the smoothing of the images.

It has been reported that brain atrophy is present in cirrhosis patients<sup>[16]</sup> and that comparison of atrophied and normal brains may lead to systematic errors<sup>[17]</sup>. To assess, whether atrophy interferes with voxel-based analysis in patients with liver cirrhosis, a test with binary images was performed. Binary images were generated from the normalized images of all patients and controls using MRIcro-Software. Pixels that contained brain were given the value 1. Pixels that contained cerebrospinal fluid (CSF) were set to 0.

### Statistical analysis

Statistical mapping analysis has been applied in functional brain imaging [fMRI or positron emission tomography (PET)]. Recently, the method's successful use has been demonstrated in diffusion-weighted imaging<sup>[18]</sup>, fluid-attenuated inversion-recovery imaging<sup>[19]</sup>, perfusion-weighted imaging<sup>[20]</sup> and MTI<sup>[21]</sup>.

We conducted a voxel-based analysis using the statistical non-parametric mapping (SnPM5b) software<sup>[22]</sup> based on SPM5<sup>[15]</sup>. A non-parametric approach was chosen because uniform variance across the volumes was not given and group size did not permit parametric tests. SnPM uses a permutation approach to account

for the multiple comparison problem in voxel-by-voxel evaluation. It does not make the assumptions derived from random field theory underlying the multiple comparison corrections used in SPM<sup>[22]</sup>.

For all statistical models employed, a threshold of  $P < 0.001$  was used to determine significance. Non-parametric testing was conducted with 10000 random permutations when possible permutations exceeded this number. The anatomical localization of the maximum statistics was determined by co-examination of the SnPM (pseudo-)t map and the customized MTR template. The results are displayed as SnPM (pseudo-)t-map images superimposed on MTR maps of representative subjects.

Based on the hypothesis that cirrhosis patients (no HE, mHE, HE 1 and HE 2) had lower MTR values than controls, two-sample, one-sided permutation tests were conducted. Subject age was included as a confounder in the group comparison tests. Correlation between the MTR maps and CFF was tested. The binary images were tested on the hypothesis of a decreased brain volume in cirrhosis patients compared with controls.

## RESULTS

### MTR group comparisons

Compared with controls, cirrhosis patients without neurological deficits (no HE) displayed significantly decreased MTR values in the basal ganglia and in the hemispheric white matter (Table 2). The maximum statistics were located in the right putamen [(pseudo-)  $t = 4.60$ ,  $P = 0.0004$ ] (Figure 2). Statistics in the left putamen were (pseudo-)  $t = 2.65$ ,  $P = 0.0006$ . In the group with mHE, a significant MTR decrease was found in hemispheric white matter, deep grey matter, brainstem and cerebellum. The cluster exhibiting the maximum statistics was in the right putamen (pseudo-)  $t = 8.57$ ,  $P = 0.0008$ . Contralateral statistics were [(pseudo-)  $t = 5.72$ ,  $P = 0.0004$ ].

The groups with overt HE showed an MTR decrease in the entire brain. In HE 1, the maximum statistics were detected in the left posterior white matter [(pseudo-)  $t = 8.82$ ,  $P = 0.0001$ ]. The statistics of the right posterior white matter were (pseudo-)  $t = 4.70$ ,  $P = 0.0001$ . In HE 2, the maximum statistics were found in the left globus pallidus [(pseudo-)  $t = 17.98$ ,  $P = 0.0001$ ]. The statistics of the right globus pallidus were (pseudo-)  $t = 14.06$ ,  $P = 0.0001$ .

### Binary data comparison

The SnPM results showed significant differences in external and internal CSF space between cirrhosis patients and controls (Figure 3). Spatial extent and maximum (pseudo-)  $t$  was higher in the patients with overt HE.

### Correlation of CFF and MTR

In the cirrhosis patients, a positive correlation between CFF and MTR was found in basal ganglia and in supra- and infratentorial white matter (Figures 4 and 5, Table 3). Largest statistics detected in a brain parenchyma cluster

**Table 2** Patients with no HE, mHE, HE 1 and HE 2 compared to controls (SnPM two-sample *t* test)

	Cluster level		Voxel level			SPM coordinates (mm)		
	k	<i>P</i> (FWE corrected)	<i>P</i> (FDR corrected)	(Pseudo-) <i>t</i>	<i>P</i> (uncorrected)	x	y	z
Controls vs no HE	209966	0.4753	0.5034	4.60	0.0004	-53	18	38
		0.7301	0.5034	4.27	0.0019	32	-101	-14
		0.8160	0.5034	4.14	0.0002	-27	17	55
Controls vs mHE	2652240	0.0045	0.0140	8.57	0.0008	-8	54	1
		0.0090	0.0140	8.27	0.0008	37	18	32
		0.0135	0.0140	7.72	0.0008	-19	-40	40
Controls vs HE 1	288720	0.0003	0.0034	8.82	0.0001	-38	-74	1
		0.0010	0.0034	8.31	0.0001	-38	-59	-10
		0.0017	0.0034	7.91	0.0001	-30	-26	1
Controls vs HE 2	286240	0.0001	0.0006	17.98	0.0001	22	-6	-6
		0.0001	0.0005	14.33	0.0001	-19	-38	36
		0.0001	0.0005	14.31	0.0001	18	2	-4

k: Number of voxels in significant clusters; FWE: Family-wise error; FDR: False discovery rate corrected and uncorrected; *P* and SnPM (pseudo-)*t* of most significant voxel clusters and their coordinates.

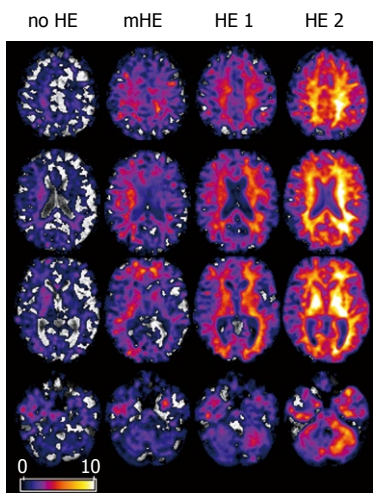


**Figure 2 (Pseudo-)*t*-maps.** MTR of patients with no HE, mHE, HE 1 and HE 2 compared to controls. Axial views superimposed on MTR maps of representative subjects. Colored areas represent voxels with significant decrease in MTR. Grey and white matter are involved. Local statistical maxima were found in basal ganglia and posterior white matter.

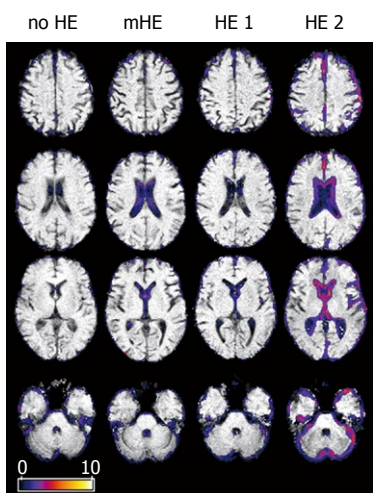


**Figure 3 (Pseudo-)*t*-maps.** Binary data of patients with no HE, mHE, HE 1 and HE 2 compared to controls. Axial views superimposed on the binary images of representative subjects showing differences in brain size. Colored areas represent voxels with significant differences. CSF space was increased in lateral cerebral fissure; parietal, frontal and cerebellar gyration were prominent in overt HE.

were in the left frontal white matter: (pseudo-)*t* = 7.06, *P* = 0.0001. Contralateral frontal white matter statistics were (pseudo-)*t* = 4.11, *P* = 0.0004.

**DISCUSSION**

MTI is an application of MRI that is used to assess non-water components in tissue. As opposed to conventional

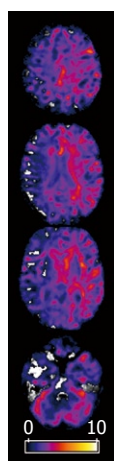


**Figure 4 (Pseudo-)*t*-maps (*P* < 0.001).** Areas with a correlation of subjects' CFF and MTR. Axial views superimposed on the MTR map of a representative subject (mHE). Colored areas represent voxels with significant positive correlation between CFF and MTR. The maximum statistics of a brain parenchyma cluster were found in left frontal white matter.

MRI, which is designed to represent different relaxation times in different tissues, MTI uses the exchange of magnetic properties between two brain tissue components: free water and macromolecules. Magnetization transfer takes place with and without physical exchange of protons between these two components. The extent of magnetization transfer is quantified using the ratio between two MR images. One image is acquired without and one with a high-frequency pulse that is designed to saturate the macromolecules. This results in a signal difference between the two images, as a result of the transfer of magnetization from free water protons towards macromolecules. The index derived from the two images can be calculated pixelwise and is rendered as an MTR map<sup>[23]</sup>. Changes in both components can lead to abnormal magnetization transfer. Depletion of macromolecules, a different macromolecule composition, as well as changes in brain water content may influence MTR.

Abnormal magnetization transfer is a known pathological feature in MRI of HE<sup>[24]</sup>. It has been reported to increase with the severity of HE. The present study provides a description of the distribution of these changes. In comparison to former studies that rely on simple ROI type analysis, a voxel-based approach was used to detect the localization of magnetization transfer changes in HE.

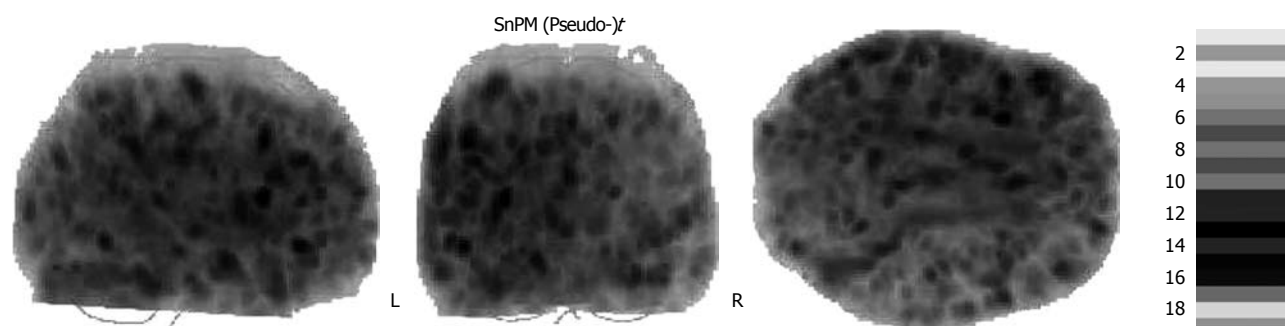


**Figure 5 (Pseudo-)t results ( $P < 0.001$ ).** Voxel clusters with a correlation of subjects' CFF and MTR. SnPM glass brain representation of voxel clusters with a positive correlation between CFF and MTR (sagittal, coronal and axial view). A significant correlation was seen in all lobes.

**Table 3 Correlation of MTR and CFF (SnPM  $t$  test)**

	Cluster level	Voxel level				SPM coordinates (mm)		
	k	$P$ (FWE corrected)	$P$ (FDR corrected)	(Pseudo-)t	$P$ (uncorrected)	x	y	z
Controls vs no HE	280567	0.0031	0.0137	7.06	0.0001	-34	18	8
		0.0167	0.0137	6.26	0.0001	-53	18	38
		0.0205	0.0137	6.19	0.0001	-54	35	-17

### Spatial distribution of MTR abnormalities

MTR reduction in the brain of patients with cirrhosis involved white and grey matter, the brainstem and the cerebellum. The MTR decrease was more severe in patients with overt HE. The area of significantly reduced MTR was larger in patients with severe HE.

These results go beyond the findings of Iwasa *et al*<sup>[5]</sup>, who have reported decreased MTR values in anatomically defined areas of the brain (globus pallidus, putamen, thalamus, corona radiata and subcortical white matter) in 37 cirrhosis patients with mHE, compared to controls. They also support and exceed the reports of Córdoba *et al*<sup>[6]</sup>, Rovira *et al*<sup>[7]</sup> and Balata *et al*<sup>[9]</sup>, who have described a loss of magnetization transfer effect in frontal and parietal white matter. In patients without overt HE, the maximum statistics were in the right basal ganglia. Patients with HE 2 had a more severe loss of MTR, which was localized bilaterally and symmetrically.

The data suggest that encephalopathy in patients with liver cirrhosis is unlikely to be related to structural damage of a specific area of the brain. In the dysmetabolic situation that accompanies hepatic insufficiency, our data show a diffuse pattern of brain involvement.

Pathological MRI of basal grey matter in HE has been described before the advent of MTI. Hyperintensity in T1-weighted imaging in the globus pallidus of patients with cirrhosis is a frequent finding<sup>[25]</sup>. Basal ganglia hyperintensity has been demonstrated to be reversible after successful liver transplantation<sup>[26]</sup>. Manganese deposition is a suggested condition to shorten T1 in the basal ganglia of cirrhosis patients<sup>[3,27]</sup>, and to be an additive factor to the extrapyramidal symptoms in these patients<sup>[28]</sup>. In the mouse brain, significant shortening of T1 relaxation can be demonstrated after intravenous, intraperitoneal or subcutaneous administration of MnCl<sub>2</sub><sup>[29]</sup>. In a quantitative T1-mapping study of the brains of patients with liver cirrhosis and HE, Shah *et al*<sup>[30]</sup> have

reported T1-shortening for the globus pallidus, caudate nucleus, and posterior limb of the internal capsule. They have discussed manganese deposition as a possible reason for their findings. No significant correlation between HE severity and T1 relaxation time could be found in the putamen, frontal white matter, white matter of the corona radiata, white matter in the occipital lobe, the anterior limb of the internal capsule, visual cortex, thalamus, or frontal cortex<sup>[30]</sup>. Patients with stage 1-2 primary biliary cirrhosis have been shown to exhibit a decrease in pallidal MTR (normalized to putamen), which correlates with blood manganese concentration<sup>[31]</sup>.

In a study of diffusion-weighted imaging, Lodi *et al*<sup>[32]</sup> have reported increased diffusivity in white matter and basal ganglia, which suggests the presence of brain edema in chronic hepatic failure<sup>[32]</sup>. Increased diffusion in mHE and overt HE has been demonstrated to be reversible after successful treatment<sup>[33]</sup>. Both edema and manganese deposition may be explanations for the decrease in magnetization transfer effect.

White matter involvement in HE may be an effect of disturbed blood flow and energy metabolism<sup>[9]</sup>, demyelination<sup>[5]</sup>, axonal loss<sup>[5]</sup>, as well as an effect of astrocytic water retention<sup>[5-7,9,10]</sup>. The loss in magnetization transfer reflected in a decrease in MTR has been proposed to be associated with brain edema in neuropsychiatric systemic lupus erythematosus<sup>[34]</sup>, multiple sclerosis<sup>[35]</sup> and traumatic brain injury<sup>[36]</sup>. In non-cirrhotic patients with portal vein thrombosis, decreased MTR values of normal-appearing white matter have been found, which has been interpreted as an increase in free brain water<sup>[37]</sup>.

The presence of white matter edema in chronic liver dysfunction is supported by the above findings of Lodi *et al*<sup>[32]</sup> and Kale *et al*<sup>[33]</sup>, who reported increased diffusivity in white matter areas and in the basal ganglia.

MR spectroscopy has established the presence of a disturbed metabolic pattern in cirrhosis, which is considered

to represent a state of minimal brain swelling<sup>[26,38,39]</sup>. Reversibility after successful liver transplantation has been suggested to be an indicator of increased free cerebral water rather than structural damage<sup>[8]</sup>.

The maximum statistics in the groups without overt HE were in the right putamen. In patients with HE 1 and HE 2, the highest (pseudo-)  $t$  was located in the left hemisphere. In each of the four groups, the corresponding contralateral brain area exhibited strongly significant, yet slightly lower statistics. The limited group size and the lack of information about the patients' handedness hinder interpretation of this finding. Unilateral brain involvement is unlikely under dysmetabolic conditions, with clinical symptoms of lack of awareness, constructional apraxia, dyscalculia, personality change and asterixis. A non-focal alteration of the dominant hemisphere might be expected to yield a stronger correlation with neuropsychological test results, than the same alteration of the non-dominant hemisphere. Nevertheless, a structurally higher susceptibility of the dominant hemisphere to metabolic toxins might be worthy of discussion. Further studies will possibly be dedicated to this question.

#### **MTI and CFF**

CFF assesses neurological deficits in cirrhosis as a continuous parameter, rather than offering the six-tier graduation used in the (revised) West-Haven criteria<sup>[40]</sup>. Since the test requires cooperation from the patients, its use in high-grade HE may be hindered. Patients suffering HE grade 3 and 4 were not enrolled in the present study. The CFF has been shown to be reliable in retest evaluation and responds rapidly to neurological deterioration or recovery<sup>[12]</sup>. Both parameters have been shown independently to decrease with increasing severity of HE<sup>[4,7,9,10,12]</sup>.

In an fMRI study, Zafiris *et al*<sup>[41]</sup> have found impaired activation of visual cortex and abnormal neuronal coupling in cirrhosis patients with decreased CFF. Alzheimer-II degeneration of glial Muller cells and mild visual impairment is another proposed mechanism of CFF decrease in HE<sup>[12]</sup>.

A positive correlation was found between CFF and cerebral MTR. Our findings indicate that the MTR of large areas of normal-appearing white matter and deep grey matter correlates with a decrease in CFF in patients with HE.

#### **Brain atrophy in HE**

SnPM group comparison of the binary data sets showed prominent sulci, ventricles and lateral cerebral fissures as morphological correlations of brain atrophy.

In normal aging, a linear decrease in brain volume is known<sup>[42]</sup>. Although there was no significant difference between the mean age of patients ( $61.1 \pm 12.4$  years) and that of the control subjects ( $55.7 \pm 13.8$  years) in the present study, subject age was included in the analysis as a confounding variable. The findings from these images point towards an effect of cirrhosis on brain volume. Brain atrophy has been reported to be present in minimal and overt HE<sup>[27]</sup>, which correlates with poor psychometric performance<sup>[16,43]</sup>.

In voxel-based analysis following normalization, the comparison of normal and atrophied brains may lead to tests, in which voxels with mainly brain parenchyma in controls are tested against voxels that contain predominantly CSF in patients. This may result in non-valid differences. The topic of using the same spatial normalization algorithm for anatomically normal and atrophied brains has been addressed by Ishii *et al*<sup>[17]</sup>. Comparing SPM and NEUROSTAT normalization methods for the analysis of PET images in Alzheimer's disease, the authors have concluded that brains with atrophy tend to show artefacts caused by the anatomical standardization process.

In an MRI and PET study of schizophrenia, SPM results were deemed invalid because of incorrect spatial normalization of atrophied brains. This led to an underestimation of metabolic activity in the caudate nucleus in patients with schizophrenia<sup>[44]</sup>.

The present work shows a correlation between MTR and CFF in intraventricular and superficial voxels. This may be attributed to unreliable normalization of brains with atrophy in the patient group. Evaluating cortical or periventricular MTR values is limited by this effect.

In conclusion, in the brains of patients with non-alcoholic liver cirrhosis, MTR loss is seen. It involves basal ganglia and white matter, even in mild stages of HE. The changes are more severe and spatially more extended in patients with HE. Maximum statistics were found in the basal ganglia in overt HE, compared to healthy controls. The correlation of MTR and CFF is strongest in frontal white matter. Analyses of cerebral MTI of patients with liver cirrhosis might profit from inclusion of both basal ganglia and frontal white matter.

## **COMMENTS**

### **Background**

Hepatic encephalopathy (HE) is a frequent complication of liver cirrhosis and is associated with poor prognosis. Many studies have shown that magnetization transfer imaging (MTI) of the brain is sensitive to HE and subclinical forms of this condition [minimal HE (mHE)]. Treatment as well as induction of HE has been monitored successfully with MTI. Edema with water accumulation is a possible mechanism for MTI changes. Many brain areas have been investigated with MTI, but no systematic evaluation of the spatial pattern of MTI abnormalities in HE has been published.

### **Research frontiers**

In the area of brain imaging in liver cirrhosis, the research hotspot is whether magnetic resonance imaging (MRI) can be used to detect HE early and to monitor its treatment. MTI is a MRI technique that is used to assess the interaction of free water protons and macromolecules. MTI is a promising research tool to assess minimal brain edema in HE.

### **Innovations and breakthroughs**

In the previous application of MTI in HE, alterations have been reported for various brain areas such as the frontal and posterior white matter, basal ganglia and thalamus. More recent studies have demonstrated the sensitivity of MTI in mHE. These studies used simple region-of-interest (ROI) evaluations. The selection of ROIs was based on *a priori* assumptions from reports on white matter MRI anomalies and manganese deposits in the basal ganglia. To the best of the authors' knowledge, no systematic assessment of the distribution of brain MTI changes has been published on which to base the selection of ROIs in the imaging of HE. In the present study, they performed a voxel-based analysis (VBA) of MTI data of patients with HE and showed that abnormal signals were present throughout the brain. No one specific area was present where MTI changes in manifest HE were exclusive.

## Applications

The study results suggest that MTI changes in HE are present throughout the brain. Test results in frontal and posterior white matter, thalamus and basal ganglia were statistically significant in cases with mHE, which might be areas that could be used as ROIs in monitoring HE by means of MTI.

## Terminology

HE is a neurological condition with fatigue, sleeping disorders and motor deficits caused by liver cirrhosis. MTI is an MRI technique that is used to assess the interaction of free water protons and macromolecules, e.g. in mild brain edema. ROI is a means of evaluating MR images of the brain by measuring an image parameter in a defined area. VBA is a statistical evaluation of the entire brain MRI data of a study population.

## Peer review

The manuscript entitled "Voxel-based analyses of magnetization transfer imaging of the brain in hepatic encephalopathy" is an interesting study that aimed to evaluate the spatial distribution of cerebral abnormalities in cirrhosis patients with and without HE found in MTI.

## REFERENCES

- 1 **Gitlin N**, Lewis DC, Hinkley L. The diagnosis and prevalence of subclinical hepatic encephalopathy in apparently healthy, ambulant, non-shunted patients with cirrhosis. *J Hepatol* 1986; **3**: 75-82
- 2 **Rink C**, Haeting J, Nilius R. Prognosis assessment in patients with liver cirrhosis [Abstract]. *Hepatogastroenterology* 1990; **37** (suppl II): 5144
- 3 **Taylor-Robinson SD**, Oatridge A, Hajnal JV, Burroughs AK, McIntyre N, deSouza NM. MR imaging of the basal ganglia in chronic liver disease: correlation of T1-weighted and magnetisation transfer contrast measurements with liver dysfunction and neuropsychiatric status. *Metab Brain Dis* 1995; **10**: 175-188
- 4 **Iwasa M**, Kinosada Y, Watanabe S, Furuta M, Yuda H, Kawamura N, Nakayabu M, Esaki A, Sato T, Deguchi T, Nakatsuka A, Adachi Y. Hepatic cirrhosis: magnetisation transfer contrast in the globus pallidus. *Neuroradiology* 1998; **40**: 145-149
- 5 **Iwasa M**, Kinosada Y, Nakatsuka A, Watanabe S, Adachi Y. Magnetization transfer contrast of various regions of the brain in liver cirrhosis. *AJNR Am J Neuroradiol* 1999; **20**: 652-654
- 6 **Córdoba J**, Alonso J, Rovira A, Jacas C, Sanpedro F, Castells L, Vargas V, Margarit C, Kulisevsky J, Esteban R, Guardia J. The development of low-grade cerebral edema in cirrhosis is supported by the evolution of (1)H-magnetic resonance abnormalities after liver transplantation. *J Hepatol* 2001; **35**: 598-604
- 7 **Rovira A**, Grivé E, Pedraza S, Rovira A, Alonso J. Magnetization transfer ratio values and proton MR spectroscopy of normal-appearing cerebral white matter in patients with liver cirrhosis. *AJNR Am J Neuroradiol* 2001; **22**: 1137-1142
- 8 **Rovira A**, Córdoba J, Sanpedro F, Grivé E, Rovira-Gols A, Alonso J. Normalization of T2 signal abnormalities in hemispheric white matter with liver transplant. *Neurology* 2002; **59**: 335-341
- 9 **Balata S**, Olde Damink SW, Ferguson K, Marshall I, Hayes PC, Deutz NE, Williams R, Wardlaw J, Jalan R. Induced hyperammonemia alters neuropsychology, brain MR spectroscopy and magnetization transfer in cirrhosis. *Hepatology* 2003; **37**: 931-939
- 10 **Miese F**, Kircheis G, Wittsack HJ, Wenserski F, Hemker J, Mödder U, Häussinger D, Cohnen M. 1H-MR spectroscopy, magnetization transfer, and diffusion-weighted imaging in alcoholic and nonalcoholic patients with cirrhosis with hepatic encephalopathy. *AJNR Am J Neuroradiol* 2006; **27**: 1019-1026
- 11 **Pugh RN**, Murray-Lyon IM, Dawson JL, Pietroni MC, Williams R. Transection of the oesophagus for bleeding oesophageal varices. *Br J Surg* 1973; **60**: 646-649
- 12 **Kircheis G**, Wettstein M, Timmermann L, Schnitzler A, Häussinger D. Critical flicker frequency for quantification of low-grade hepatic encephalopathy. *Hepatology* 2002; **35**: 357-366
- 13 **Jalan R**, Hayes PC. Hepatic encephalopathy and ascites. *Lancet* 1997; **350**: 1309-1315
- 14 **Smith SM**. Fast robust automated brain extraction. *Hum Brain Mapp* 2002; **17**: 143-155
- 15 **Friston KJ**, Holmes AP, Worsley KJ, Poline JP, Frith CD, Frackowiak RSJ. Statistical parametric maps in functional imaging: A general linear approach. *Hum Brain Mapp* 1995; **2**: 189-210
- 16 **Amodio P**, Pellegrini A, Amistà P, Luise S, Del Piccolo F, Mapelli D, Montagnese S, Musto C, Valenti P, Gatta A. Neuropsychological-neurophysiological alterations and brain atrophy in cirrhotic patients. *Metab Brain Dis* 2003; **18**: 63-78
- 17 **Ishii K**, Willoch F, Minoshima S, Drzezga A, Ficarò EP, Cross DJ, Kuhl DE, Schwaiger M. Statistical brain mapping of 18F-FDG PET in Alzheimer's disease: validation of anatomic standardization for atrophied brains. *J Nucl Med* 2001; **42**: 548-557
- 18 **Chappell MH**, Uluğ AM, Zhang L, Heitger MH, Jordan BD, Zimmerman RD, Watts R. Distribution of microstructural damage in the brains of professional boxers: a diffusion MRI study. *J Magn Reson Imaging* 2006; **24**: 537-542
- 19 **Focke NK**, Symms MR, Burdett JL, Duncan JS. Voxel-based analysis of whole brain FLAIR at 3T detects focal cortical dysplasia. *Epilepsia* 2008; **49**: 786-793
- 20 **Rashid W**, Parkes LM, Ingle GT, Chard DT, Toosy AT, Altmann DR, Symms MR, Tofts PS, Thompson AJ, Miller DH. Abnormalities of cerebral perfusion in multiple sclerosis. *J Neurol Neurosurg Psychiatry* 2004; **75**: 1288-1293
- 21 **Audoin B**, Ranjeva JP, Au Duong MV, Ibarrola D, Malikova I, Confort-Gouny S, Soulier E, Viout P, Ali-Chérif A, Pelletier J, Cozzzone PJ. Voxel-based analysis of MTR images: a method to locate gray matter abnormalities in patients at the earliest stage of multiple sclerosis. *J Magn Reson Imaging* 2004; **20**: 765-771
- 22 **Nichols TE**, Holmes AP. Nonparametric permutation tests for functional neuroimaging: a primer with examples. *Hum Brain Mapp* 2002; **15**: 1-25
- 23 **McGowan JC**. The physical basis of magnetization transfer imaging. *Neurology* 1999; **53**: S3-S7
- 24 **Grover VP**, Dresner MA, Forton DM, Counsell S, Larkman DJ, Patel N, Thomas HC, Taylor-Robinson SD. Current and future applications of magnetic resonance imaging and spectroscopy of the brain in hepatic encephalopathy. *World J Gastroenterol* 2006; **12**: 2969-2978
- 25 **Inoue E**, Hori S, Narumi Y, Fujita M, Kuriyama K, Kadota T, Kuroda C. Portal-systemic encephalopathy: presence of basal ganglia lesions with high signal intensity on MR images. *Radiology* 1991; **179**: 551-555
- 26 **Naegele T**, Grodd W, Viebahn R, Seeger U, Klose U, Seitz D, Kaiser S, Mader I, Mayer J, Lauchart W, Gregor M, Voigt K. MR imaging and (1)H spectroscopy of brain metabolites in hepatic encephalopathy: time-course of renormalization after liver transplantation. *Radiology* 2000; **216**: 683-691
- 27 **Zeneroli ML**, Cioni G, Crisi G, Vezzelli C, Ventura E. Globus pallidus alterations and brain atrophy in liver cirrhosis patients with encephalopathy: an MR imaging study. *Magn Reson Imaging* 1991; **9**: 295-302
- 28 **Butterworth RF**, Spahr L, Fontaine S, Layrargues GP. Manganese toxicity, dopaminergic dysfunction and hepatic encephalopathy. *Metab Brain Dis* 1995; **10**: 259-267
- 29 **Kuo YT**, Herlihy AH, So PW, Bhakoo KK, Bell JD. In vivo measurements of T1 relaxation times in mouse brain associated with different modes of systemic administration of manganese chloride. *J Magn Reson Imaging* 2005; **21**: 334-339
- 30 **Shah NJ**, Neeb H, Zaitsev M, Steinhoff S, Kircheis G, Amunts K, Häussinger D, Zilles K. Quantitative T1 mapping of hepatic encephalopathy using magnetic resonance imaging. *Hepatology* 2003; **38**: 1219-1226
- 31 **Forton DM**, Patel N, Prince M, Oatridge A, Hamilton G, Goldblatt J, Allsop JM, Hajnal JV, Thomas HC, Bassendine M,

- Jones DE, Taylor-Robinson SD. Fatigue and primary biliary cirrhosis: association of globus pallidus magnetisation transfer ratio measurements with fatigue severity and blood manganese levels. *Gut* 2004; **53**: 587-592
- 32 **Lodi R**, Tonon C, Stracciari A, Weiger M, Camaggi V, Iotti S, Donati G, Guarino M, Bolondi L, Barbiroli B. Diffusion MRI shows increased water apparent diffusion coefficient in the brains of cirrhotics. *Neurology* 2004; **62**: 762-766
- 33 **Kale RA**, Gupta RK, Saraswat VA, Hasan KM, Trivedi R, Mishra AM, Ranjan P, Pandey CM, Narayana PA. Demonstration of interstitial cerebral edema with diffusion tensor MR imaging in type C hepatic encephalopathy. *Hepatology* 2006; **43**: 698-706
- 34 **Emmer BJ**, Steens SC, Steup-Beekman GM, van der Grond J, Admiraal-Behloul F, Olofsen H, Bosma GP, Ouwendijk WJ, Huizinga TW, van Buchem MA. Detection of change in CNS involvement in neuropsychiatric SLE: a magnetization transfer study. *J Magn Reson Imaging* 2006; **24**: 812-816
- 35 **Hähnel S**, Münkler K, Jansen O, Heiland S, Reidel M, Freund M, Aschoff A, Sartor K. Magnetization transfer measurements in normal-appearing cerebral white matter in patients with chronic obstructive hydrocephalus. *J Comput Assist Tomogr* 1999; **23**: 516-520
- 36 **Bagley LJ**, Grossman RI, Galetta SL, Sinson GP, Kotapka M, McGowan JC. Characterization of white matter lesions in multiple sclerosis and traumatic brain injury as revealed by magnetization transfer contour plots. *AJNR Am J Neuroradiol* 1999; **20**: 977-981
- 37 **Mínguez B**, García-Pagán JC, Bosch J, Turnes J, Alonso J, Rovira A, Córdoba J. Noncirrhotic portal vein thrombosis exhibits neuropsychological and MR changes consistent with minimal hepatic encephalopathy. *Hepatology* 2006; **43**: 707-714
- 38 **Kreis R**, Ross BD, Farrow NA, Ackerman Z. Metabolic disorders of the brain in chronic hepatic encephalopathy detected with H-1 MR spectroscopy. *Radiology* 1992; **182**: 19-27
- 39 **Ross BD**, Jacobson S, Villamil F, Korula J, Kreis R, Ernst T, Shonk T, Moats RA. Subclinical hepatic encephalopathy: proton MR spectroscopic abnormalities. *Radiology* 1994; **193**: 457-463
- 40 **Conn HO**. Subclinical hepatic encephalopathy. In: Bircher J, editor. *Hepatic encephalopathy: syndromes and therapies*. Bloomington: Medi-ed Press, 1994: 27-42
- 41 **Zafiris O**, Kircheis G, Rood HA, Boers F, Häussinger D, Zilles K. Neural mechanism underlying impaired visual judgement in the dysmetabolic brain: an fMRI study. *Neuroimage* 2004; **22**: 541-552
- 42 **Good CD**, Johnsrude IS, Ashburner J, Henson RN, Friston KJ, Frackowiak RS. A voxel-based morphometric study of ageing in 465 normal adult human brains. *Neuroimage* 2001; **14**: 21-36
- 43 **Moore JW**, Dunk AA, Crawford JR, Deans H, Besson JA, De Lacey G, Sinclair TS, Mowat NA, Brunt PW. Neuropsychological deficits and morphological MRI brain scan abnormalities in apparently healthy non-encephalopathic patients with cirrhosis. A controlled study. *J Hepatol* 1989; **9**: 319-325
- 44 **Reig S**, Penedo M, Gispert JD, Pascau J, Sánchez-González J, García-Barreno P, Desco M. Impact of ventricular enlargement on the measurement of metabolic activity in spatially normalized PET. *Neuroimage* 2007; **35**: 748-758

S- Editor Tian L L- Editor Kerr C E- Editor Zheng XM